Ureter Tracking and Segmentation in CT Urography (CTU) using COMPASS

Lubomir Hadjiiski,
David Zick,
Heang-Ping Chan,
Richard H. Cohan,
Elaine M. Caoili,
Kenny Cha,
Chuan Zhou,
Jun Wei

Department of Radiology, University of Michigan, Ann Arbor, MI

Running Title: Ureter Segmentation in CT Urography (CTU) using COMPASS

Correspondence:

Lubomir Hadjiiski, Ph.D.
Department of Radiology
University of Michigan
1500 E. Medical Center Drive
MIB C476
Ann Arbor, MI 48109-5842
Telephone: (734) 647-7428
Fax: (734) 615-5513
E-mail: lhadjisk@umich.edu

ABSTRACT

Purpose: We are developing a computerized system for automated segmentation of ureters in CTU, referred to as COmbined Model-guided Path-finding Analysis and Segmentation System (COMPASS). Ureter segmentation is a critical component for computer-aided diagnosis of ureter cancer.

Methods: COMPASS consists of three stages: (1) rule-based adaptive thresholding and region growing, (2) path-finding and propagation, and (3) edge profile extraction and feature analysis. With IRB approval, 79 CTU scans performed with intravenous (IV) contrast material enhancement were collected retrospectively from 79 patient files. One hundred twenty-four ureters were selected from the 79 CTU volumes. On average, the ureters spanned 283 CT slices (range: 116 to 399, median: 301). More than half of the ureters contained malignant or benign lesions and some had ureter wall thickening due to malignancy. A starting point for each of the 124 ureters was identified manually to initialize the tracking by COMPASS. In addition, the centerline of each ureter was manually marked and used as reference standard for evaluation of tracking performance. The performance of COMPASS was quantitatively assessed by estimating the percentage of the length that was successfully tracked and segmented for each ureter, and by estimating the average distance and the average maximum distance between the computer and manually tracked centerlines.

Results: Of the 124 ureters, 120 (97%) were segmented completely (100%), 121 (98%) were segmented through at least 70%, and 123 (99%) were segmented through at least 50% of its length. In comparison, using our previous method, 85 (69%) ureters were segmented completely (100%), 100 (81%) were segmented through at least 70%, and 107 (86%) were segmented at least 50% of its length. With COMPASS, the average distance between the computer and manually generated centerlines is 0.54 mm, and the average maximum distance is 2.02 mm. With our previous method, the average distance between the centerlines was 0.80 mm, and the average maximum distance was

3.38 mm. The improvements in the ureteral tracking length and both distance measures were statistically significant ($p<0.0001$).

Conclusions: COMPASS improved significantly the ureter tracking, including regions across ureter lesions, wall thickening and the narrowing of the lumen.

Key Words: Computer-Aided Diagnosis, CT Urography, Segmentation, Model-Guided Image Analysis System, Ureter, Malignancy.

1. INTRODUCTION

Urothelial carcinoma can cause substantial morbidity and mortality among affected patients. Bladder and upper urinary tract urothelial cancer causes 16,500 deaths per year in the United States [1]. It is expected that 77,700 new bladder and upper urinary tract cancer cases will be diagnosed in 2014. Early detection of urothelial carcinoma is important; the survival rate for patients whose cancers are detected and treated early is high. When diagnosed at a localized stage, the 5-year survival is 92%. However, only 75% of cancers are detected at an early stage. When there is regional and distant metastatic disease, 5-year survival decreases to 45% and 6%, respectively. In addition, urinary tract neoplasms may be multifocal and, in such cases, all of the malignancies have to be detected and each has to be treated individually. If a malignancy is left untreated, it will eventually develop to a more advanced stage, thereby reducing the chance of survival for the patient. Therefore, early diagnosis and treatment of these lesions is crucial for reducing the morbidity, mortality and their attendant costs compared to diagnosis at a later, more symptomatic, stage when deep invasion and/or metastasis may develop.

Multi-detector row CT urography (CTU) is a useful imaging modality for evaluation of urothelial neoplasms[2-5] CTU offers the distinct advantage of providing essentially complete imaging of the urinary tract and of the abdomen and pelvis in a single study. While, in the past, patients with suspected or known urinary tract neoplasms were often imaged with combinations of intravenous pyelography (IVP), ultrasound, routine abdominal CT, and even MRI, with CTU the need for other imaging studies has been substantially reduced. CTU, therefore, has spared patients from undergoing a potentially large number of alternative imaging studies, thereby reducing health care costs.

A preliminary study[6] has suggested that CTU may have superior sensitivity in detecting urinary tract lesions compared with alternative imaging studies. Recent research has demonstrated that CTU can detect urothelial neoplasms that are extremely small (measuring as small as 2-3 mm in maximal diameter), as well as cancers that produce only thickening of the urothelium without any associated

abnormality of the urinary tract lumen. The latter is a phenomenon that was not widely known to exist until CTU began to appear. In one study, 24 of 27 subsequently diagnosed upper tract urothelial neoplasms were detected by CTU[7].

Interpretation of CTU can be a demanding task for radiologists. Each CT exam of the urinary tract produces, on average, at least 300 slices when a slice reconstruction interval of 1.25 mm is employed, with a range of 200 to 600 slices. Interpretation of a CTU exam demands extensive reading time from a radiologist who has to visually track the upper and lower urinary tract and look for tumors which are usually small in size, as well as searching obtained images for extra-urinary findings. The interpreting radiologists frequently need to adjust window settings and use zooming on a display workstation to improve visualization. Multiple lesions may exist throughout the urinary tract as well. With excreted contrast material in the urinary tract, some lesions will be in the opacified portions, while other lesions may be located adjacent to portions of the urinary tract that are unopacified at the time of imaging. This latter finding is most common in the non-dependent areas of dilated urinary tract segments. This variability makes it more challenging for the radiologists to detect urothelial neoplasms. Additionally, many different urinary tract findings may be present in any individual CT urogram. The interpreting radiologist must spend extensive time and effort identifying these findings, and then must also determine how likely each of them is an urothelial neoplasm. Techniques that would assist the radiologist in identifying areas that may contain urothelial neoplasms would be useful.

With the increase in radiologists' workload, the chance for oversight of subtle lesions may not be negligible. The application of computer-aided diagnosis (CAD) to assisting radiologists in interpretation of CTU exam may improve early detection of ureter lesions. We are developing a CAD system for detection of ureteral cancer in CTU. A critical component of such a CAD system is the accurate segmentation of the ureters from the surrounding anatomical structures. Hadjiiski et al [8] reported preliminary results for ureter segmentation in 11 patients using thresholding technique with a threshold determined from the starting seed point and applied to all CTU slices. Their algorithm

successfully tracked the ureters in 10 of the patients. In a follow-up study, Hadjiiski et al [9] applied the same algorithm to a data set of 25 ureters having good level of opacification with excreted intravenous (IV) contrast material in 20 patients. They were able to track successfully all 25 ureters. More recently, Hadjiiski et al [10] explored a new method, COmbined Model-guided Path-finding Analysis and Segmentation System (COMPASS), targeting the segmentation of more difficult cases including ureters that demonstrated a moderate level of opacification with excreted contrast material. The purpose of the current study is to further improve this computerized method for ureter tracking and segmentation in CTU exams and evaluate its performance in comparison with a reference standard.

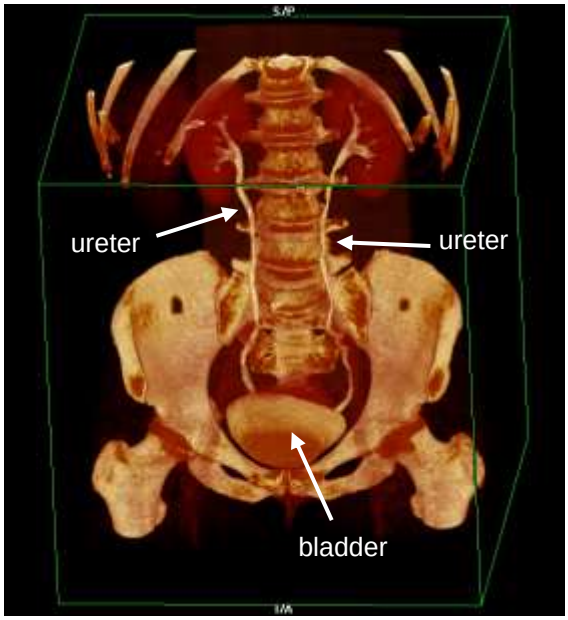

Figure 1. Volume rendering on a CTU. In this case, the ureters are clearly visible in the 3D volume. Both ureters are well opacified with IV contrast material and are seen continuously between the kidneys and the bladder.

2. MATERIALS AND METHODS

Institutional review board (IRB) approval was obtained for this retrospective study. A 3D rendering of the urinary tract from CTU is shown in Fig. 1. The ureters connect the kidneys with the bladder. Both the left and the right ureter in this case are well opacified with excreted IV contrast

material and are visible. A cross-section of the left and right ureter (from the case in Fig. 1) is shown on the axial CTU image in Fig. 2. It can be observed that the lumens of the left and right ureter have different diameters. In general, the ureter lumen diameter varies along the ureter path (Figs. 2a and 2c). More often, this variation is due to different level of ureter muscles contraction during the urine transport. If the ureteral musculature is relaxed in a specific region the corresponding ureter diameter and lumen will be larger. If the ureteral musculature is contracted the ureter diameter is very small, the lumen is narrow and often there is little, if any excreted contrast material in the ureteral lumen. The presence of a ureteral lesion or wall thickening can also cause a narrowing of the ureter lumen, which will result in a region not well opacified with excreted IV contrast material, although the ureteral wall will often be thickened. In any case, the presence of regions that are not well opacified with excreted IV contrast material and the substantial variation of the ureter diameter and lumen is a challenge for ureteral segmentation.

a b c

Figure 2. Axial CTU image and zoomed-in volume-rendered images (case shown in Fig.1) showing the left and right ureters. (a) A portion of the right ureter from the volume rendered CTU scan showing variation of the ureter diameter. (b) Axial CTU image showing the left and right ureters both well opacified with excreted IV contrast material (marked by white arrows). (c) A portion of the left ureter showing substantial variation (narrowing) of the ureter diameter.

2.1 Data set

With IRB approval, the CTU cases used in this study were collected retrospectively from patient files in the Department of Radiology. All exams were acquired with LightSpeed QX/i version 1.3, GE Healthcare MDCT scanners using an imaging technique of 120 kVp and 120–280 mA, slice interval of 0.625 mm and in-plane pixel size of 0.722 mm. They were enhanced with IV contrast material (125 - 175 mL of Omnipaque 300 [iohexol], Amersham Health, Ultravist 300 [iopromide], Bayer Healthcare, or Isovue 300 [iopamidol], Bracco) administered at a rate of 3 mL/sec, using either single-bolus or split-bolus technique. Excretory phase images were obtained beginning 12 minutes following the initial injection of contrast material. All patients received IV hydration with 250 ml of normal (0.9%) saline during their studies.

The segmentation and tracking performance was evaluated on a data set including 79 excretory phase contrast-enhanced CTU scans from 79 patients. One hundred twenty-four ureters were judged to have moderate to good level of opacification by experienced radiologists and included. Nine patients had only one ureter because of prior surgery and in 25 cases one of the ureters were judged to have poor opacification and excluded. In the cases with poor ureter opacification the ureter was opacified less than 50% of its lengths. The reasons for poor opacification were mainly lesions at the kidney or bladder blocking the ureter path and ureter inflammation. For the 124 ureters, the ureter spanned an average of 283 CT slices (range: 116 to 399, median: 301). A ureter centerline was obtained by marking manually the ureter center point on every CT slice which was used as a reference standard for evaluation of the performance of COMPASS. More than half of the ureters contained focal malignant or benign lesions and some had circumferential ureter wall thickening due to malignancy. The lesions were marked by experienced radiologists on a display workstation using an in-house developed graphic user interface (GUI). In this preliminary study, a starting point where the ureter exits the kidney was manually selected with the GUI for each of the 124 ureters, which served

as an input to COMPASS to initialize the segmentation and tracking. The distribution of the voxel gray level values in terms of Hounsfield Units (HU) for all ureters in the database is shown in Fig. 3. The mean and the range of the HU values for every ureter in the data set are shown in Fig. 4.

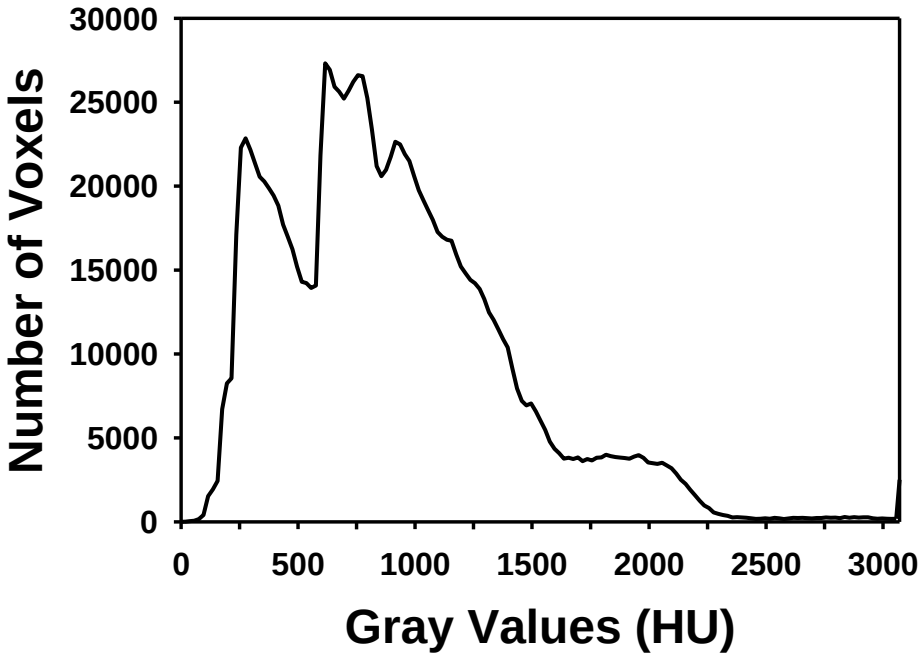

Figure 3. A distribution of the gray level values of the voxels for all ureters in the data set.

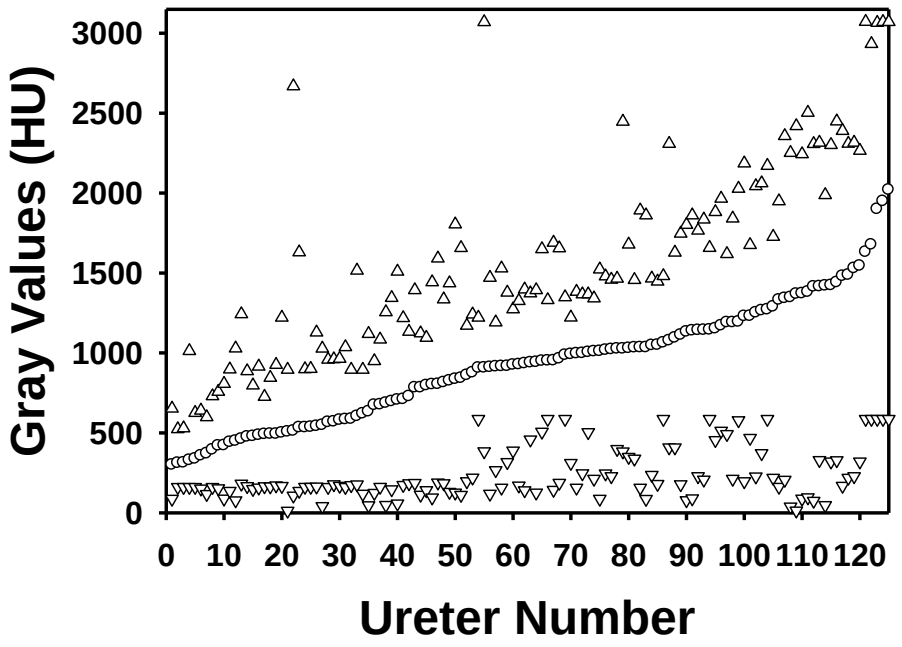

Figure 4. The mean and the range of the gray level values for every ureter in the database. The ureters in the plot are ordered based on the increasing magnitude of their mean. The range is defined as the minimum and the maximum of a ureter gray level values.

2.2 COMPASS segmentation

We have designed a COmbined Model-guided Path-finding Analysis and Segmentation System (COMPASS) for ureter segmentation. COMPASS utilizes *a priori* knowledge of the anatomical structures in CTU to track the contrast-filled lumen of ureters (Fig. 1). COMPASS consists of three stages: (1) adaptive thresholding and region growing, (2) path finding and propagation, and (3) edge profile extraction and feature analysis. Briefly, starting from an input seed point, adaptive thresholding and region growing are applied to the local region to extract the contrast-filled structure as a slice of the ureter, from which the location of the ureter in the next slice is predicted by structural connectivity. The process is guided by decision rules that incorporate the

anatomical model of the ureter such as tubular structure, connectivity, gray level contrast, size, and shape across the neighboring CTU slices. The model-guided approach imposes constraints on the path-finding process so that only the structure that has high likelihood of being the ureter will be tracked through the complex abdominal background in a CTU. A prototype of the system was described previously[10]. The prototype of the system achieved reasonable performance, segmenting cases of a range of difficulty levels including ureters that demonstrated a moderate level of opacification with excreted contrast material. However, the prototype has only one adaptive thresholding procedure, which was found to be insufficient for dealing with the large gray level variability in the data set (Fig. 3 and Fig. 4), especially for the difficult ureters with large variations in voxel gray levels and diameters. To distinguish the prototype system from the current COMPASS, the prototype will be referred to hereafter as the previous method.

2.3 Enhanced COMPASS segmentation

We have improved a number of components under the COMPASS framework. The major differences include: (1) in order to better accommodate the variable size of the ureter and enhance ureter segmentation, two adaptive thresholding loops with different decision rules were implemented in the enhanced COMPASS for ureters with smaller and larger diameters; (2) a method for generation of alternative pathway for the ureter propagation based on the structural similarity was developed; and (3) the decision rules for the estimation of the likelihood of the segmented candidate being a part of the ureter were improved. The block diagram of the enhanced COMPASS is shown in Fig. 5.

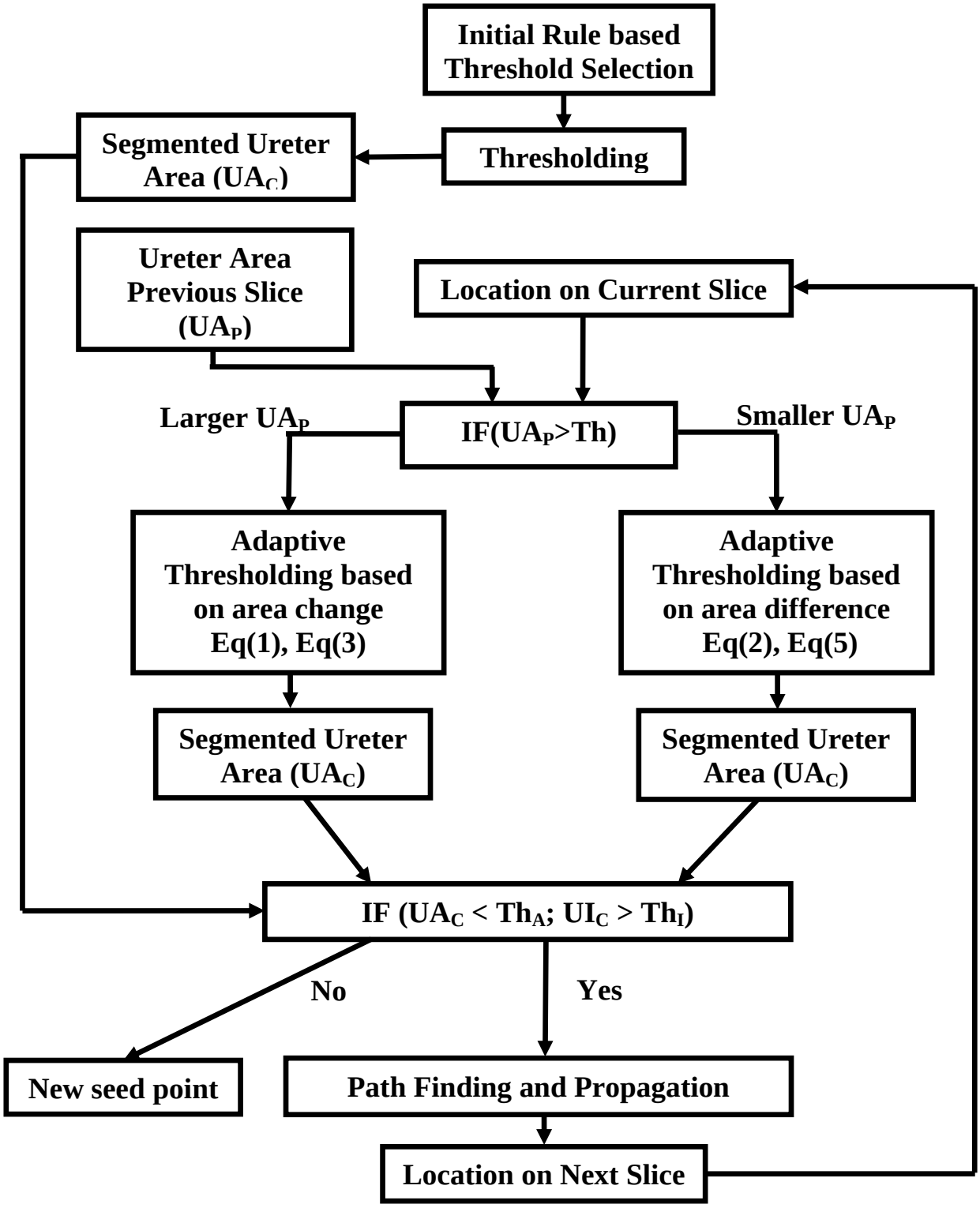

Figure 5. Block diagram of our COmbined Model-guided Path-finding Analysis and Segmentation System (COMPASS).

More detailed description of the enhanced COMPASS is presented in the following discussion. For conciseness, the enhanced COMPASS will be simply referred to as COMPASS.

For image processing purpose, all CT voxel values in terms of Hounsfield Units (HU) are linearly shifted by the relationship GL = HU+1024 so that all image voxel values are positive before being input to COMPASS although HU is used in the following discussion for its physical meaning. The segmentation procedure starts from a user-input seed point. An initial gray level threshold is determined based on the gray level intensity value of the input seed voxel. If the intensity of the input seed voxel is smaller than 976 HU the initial threshold is set to be 161 HU. In case the intensity of the input seed voxel is equal or larger than 976 HU the initial threshold is set to be 586 HU. These initial thresholds were selected experimentally to provide a segmentation of the ureter on the first slice in the majority of the cases. The gray levels of the majority of the ureter voxels were above the selected thresholds (Fig. 3 and Fig. 4). However, if the area of the segmented ureter is smaller than a predefined area of 7.8 mm^2, which was estimated from the average size of the cross section of a ureter at its origin, an adaptive adjustment of the gray level threshold is applied by subtracting 50 HU from the threshold at every iteration cycle until the area of the segmented ureter exceeds the predefined area. The path of the ureter is propagated from the current slice to the next slice with the method described below and in Fig. 5.

For further segmentation of the ureter, a rule-based adaptive thresholding procedure is used. An iterative procedure adapts the gray level threshold to keep the segmented area of the ureter close to that in the previous slice. A problem for ureter segmentation is the substantial variation of ureter diameter along its length (Fig. 2). In order to address this problem, two adaptive loops are implemented within the thresholding procedure. One loop handles ureters with larger cross-sectional area and the other handles ureters with smaller cross-sectional area in the current slice. Two criteria utilizing the

anatomical properties of the ureter were designed to control the adaptive thresholding and to manage the substantial variation of the ureter diameter.

The first criterion is based on the normalized area change (*AC*) between the segmented ureter on the previous and the current slice:

$$AC = \frac{UA_P - UA_C}{UA_P}, \tag{1}$$

where UA_P is the area of the segmented ureter on the previous slice and UA_C is the area of the segmented ureter on the current slice.

The second criterion is based on the area difference (*AD*) between the segmented ureter on the previous and the current slice:

$$AD = UA_P - UA_C \tag{2}$$

If the ureter size on the previous slice is larger than a threshold *Th* ($UA_P \geq Th$), criterion (1) *AC* is used. If the ureter size is small ($UA_P < Th$), criterion (2) *AD* is used. The value of *Th* was determined experimentally as $Th = 10.4$ mm^2 during training.

An iterative procedure adapts the gray level threshold to keep the area of the ureter close to that of the previous slice for both the smaller and the larger ureter diameters by using two optimization loops. The optimization loop for the ureters with larger cross-sectional areas updates the gray level threshold as follows:

$$Th_g(k+1) = \begin{cases} Th_g(k) - d(k) & if \quad AC > Th_{AC} \\ Th_g(k) + d(k) & if \quad AC < -Th_{AC} \end{cases}, \tag{3}$$

where Th_{AC} is the normalized area change threshold that controls the difference of the segmented ureter area on the current slice relative to that on the previous slice, $Th_g(k)$ is the gray level threshold at iteration k, and $d(k)$ is the increment or decrement of $Th_g(k)$ defined as:

$$d(k) = \begin{cases} 10 & if \quad k \leq 45 \\ 1 & if \quad k > 45 \end{cases} \tag{4}$$

The use of larger $d(k)$ value at the beginning of the optimization procedure (smaller iteration number k) allows for a faster and more reliable approach towards the global minimum by avoiding the local minima. Convergence is achieved when $|AC| \leq Th_{AC}$. However, if the convergence is not achieved for the specified iteration number (i.e. $|AC| > Th_{AC}$), the value of $d(k)$ is reduced. The smaller $d(k)$ allows for search of a local minimum and a potential convergence of the optimization procedure. Such a local minimum found after the initial global search is usually close to the global minimum. The maximum number of iterations is set to k_{max}=60, which was determined experimentally to be sufficient for the optimization loop to converge. The specific value for the area change threshold was selected experimentally as Th_{AC} = 0.4 during training.

The optimization loop for the ureters with smaller cross-sectional areas updates the gray level threshold as follows:

$$Th_g(k+1) = \begin{cases} Th_g(k) - d(k) \;\; if \quad AD > Th_{AD} \; or \; UA_C < Th_S \\ Th_g(k) + d(k) \quad if \quad AD < -Th_{AD} \end{cases}, \tag{5}$$

where Th_{AD} is the area difference threshold that controls the difference between the segmented ureter area on the current slice and that on the previous slice for small ureters, and Th_S is the minimum segmented ureter area allowed on the current slice. Convergence is achieved when $|AD| \leq Th_{AD}$ and $UA_C \geq Th_S$. The specific values for the Th_{AD} and Th_S were selected experimentally as Th_{AD} =3.6 mm^2,

and Th_S = 2.6 mm^2. $d(k)$ is defined in the same way as in Eq.(4) and the maximum number of iterations is set to k_{max}=60 as above.

The selection of the parameters in Eq.(4) was adequate for the optimization procedure to reach a solution. Fig. 6 shows the gray level threshold Th_g before and after the adaptation procedure every time when the adaptation procedure was activated for all ureters.

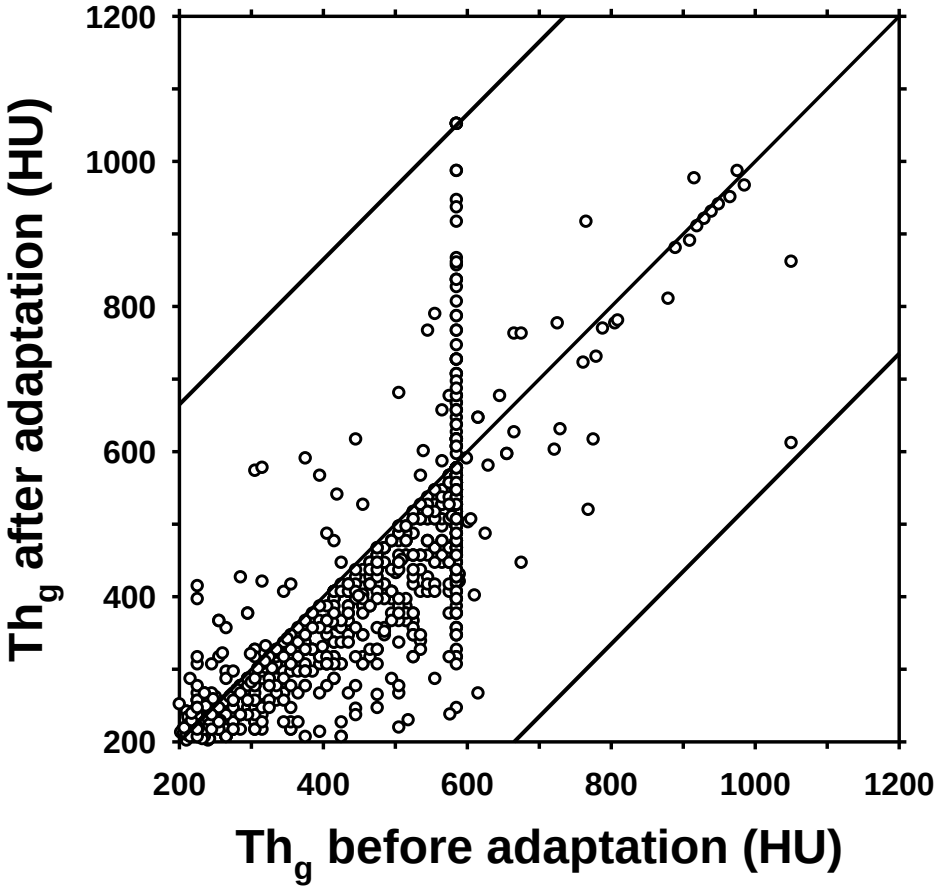

Figure 6. Gray level threshold Th_g before and after the adaptation procedure. Every circle indicates the corresponding Th_g before and after the adaptation for a single activation of the adaptation procedure. For a ureter, the adaptation procedure may be activated several times. The plot represents the total number of times when the adaptation procedure was activated for all ureters. The upper and lower lines parallel to the diagonal line represent the upper and lower bound (±465HU), respectively, of the possible change for Th_g after adaptation.

It can be observed that there was large variation in the Th_g values for the cases in our data set due to the variation in the ureter contrast levels, as shown in Fig. 3 and Fig. 4. It can also be observed that, despite the gray level variation in our data set (Fig. 3 and Fig. 4), a solution was found within the maximum number of iterations allowed (k_{max}) such that all Th_g values were within the upper and lower bound (±465 HU), as estimated by the number of iterations and the allowed step size in each iteration (=45*10+15*1), of the possible change for Th_g after adaptation.

At the next step, the ureter area, UA_C, and the average gray level intensity of the segmented area, UI_C , obtained on the current slice are compared to predefined constraint values and accepted as a part of the ureter if:

$$UA_C < Th_A \quad and \quad UI_C > Th_I \ , \tag{6}$$

where Th_A is the area constraint and Th_I is the intensity constraint. The area constraint checks whether leakage has occurred. The average gray level intensity constraint verifies whether the segmented object is sufficiently bright to be a part of a contrast-filled ureter. The specific values for the area and intensity constraints were selected experimentally as Th_A = 1042.6 mm^2 and Th_I = 226 HU during training. The COMPASS key parameter values are summarized in Table 1.

Table 1. COMPASS key parameter values.

Parameter	Value	Value (GL*)
Initial Threshold	976 HU	2000 GL
Th	10.4 mm^2	
Th_{AC}	0.4	
Th_{AD}	3.6 mm^2	
Th_S	2.6 mm^2	
k_{max}	60	
Th_A	1042.6 mm^2	
Th_I	226 HU	1250 GL

*GL = Gray Level, HU = Hounsfield Unit, HU = GL-1024

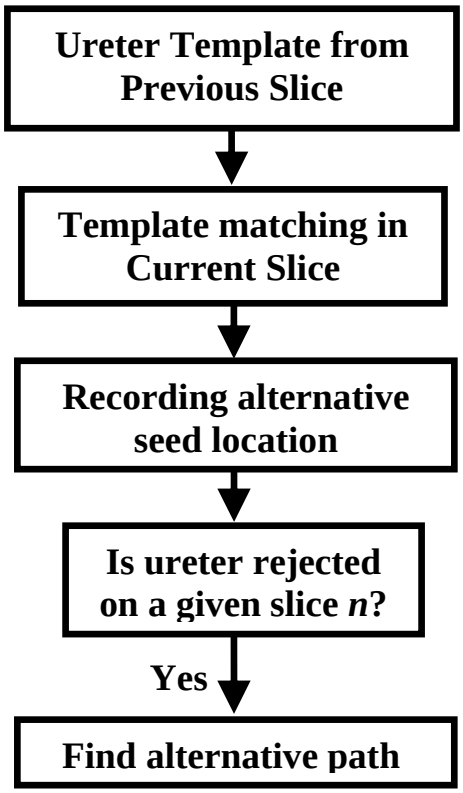

Figure 7. Block diagram of the alternative pathfinder module of COMPASS.

In case the segmented object does not satisfy the criteria in Eq. (6) and thus is not accepted as a part of the ureter, an additional procedure, referred to as the alternative pathfinder, is performed as shown in the block diagram in Fig. 7. For every current slice, a gray level image template containing the segmented ureter from the previous slice is extracted and is used for template matching within a search region that is expected to contain the ureter on the current slice. The size of the search region is chosen to be 3 times the size of the bounding box of the segmented ureter from the previous slice and centered at the same corresponding location as the ureter center in the previous slice. If the primary ureter candidate has already been found by the tracking procedure above, it is masked and excluded

during the search. The alternative ureter candidate location on the current slice is then determined by the correlation between the template and the remaining structures within the search region. The location with the maximum correlation is selected as the centroid of the second most likely ureter candidate on the current slice and is stored as an alternative seed location. This part of the alternative pathfinder procedure is applied to every CTU slice where ureter segmentation is performed. If the ureter is rejected on a given slice *n*, the alternative pathfinder will attempt ureter segmentation from the alternative seed location on the previous slice (*n*-1). If the ureter is rejected again on slice (*n*-1), the alternative pathfinder will attempt ureter segmentation from the alternative seed location on slice (*n*-2). This process can continue up to 10 previous slices (*n*-10). If the ureter is still rejected, COMPASS tracking is terminated. The alternative pathfinder provides an alternative path for tracking and helps when there are major kinks (i.e., large change in direction by an angle of more than 90^{o}, or large change in location by more than 0.5 of ureter diameter between consecutive slices) along the ureter.

Finally, the location of the ureter for the next slice is predicted by structural connectivity, i.e., the centroid of the segmented ureter on the current slice is expected to be connected to the ureter on the next slice. Therefore, it is projected to the next slice and used as the seed point for the ureter segmentation.

2.4 Performance measures

The performance of COMPASS was quantitatively assessed by three measures. The first measure was the percentage of the length that was successfully tracked. The length of a ureter was determined as the number of slices from the starting point to the end point where the ureter entered the bladder.

The second measure (*Dist*) was the distance between the COMPASS tracked and the manually generated ureter centerlines, which was defined as the Euclidean distance between the centerline points of the COMPASS tracked and the manually tracked ureters, estimated on every slice, and averaged

over all slices intersecting the segmented ureter. The average distance over all ureters was derived from the distances for the individual ureters.

The third measure was the maximum distance between the COMPASS tracked and manually generated centerlines, which was defined as the maximum of the Euclidean distances between the COMPASS tracked and the manually tracked centerline points as estimated above for an individual ureter. The average maximum distance over all ureters was derived from the maximum distances for the individual ureters.

The statistical significance of the difference in each measure between the current and the previous method was estimated by using the Student's two-tailed paired t-test.

3. RESULTS

Examples of the COMPASS segmentation and tracking of ureters are shown in Figs. 8a, 8b, 9b, 9c, and 6e.

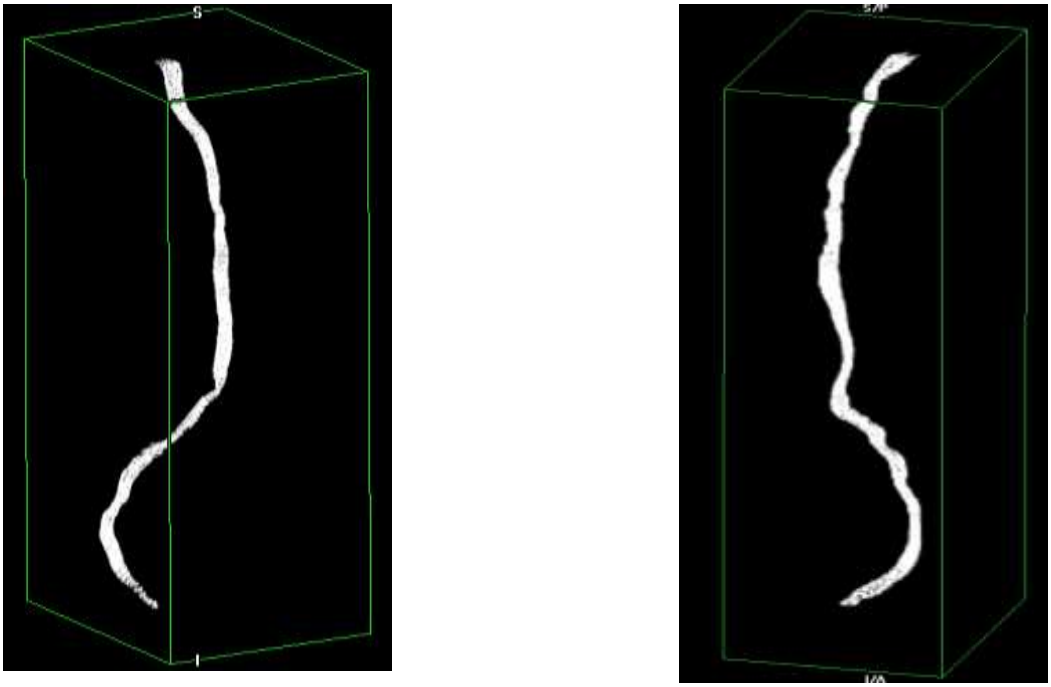

a b

Figure 8. Segmented ureters of the case from Fig.1, rendered in 3D: (a) the **right** ureter (segmented 100%, *Dist* = 0.38 mm); (b) the **left** ureter (segmented 100%, *Dist* = 0.36 mm). The sparse appearance of the voxels is caused by the volume rendering algorithm.

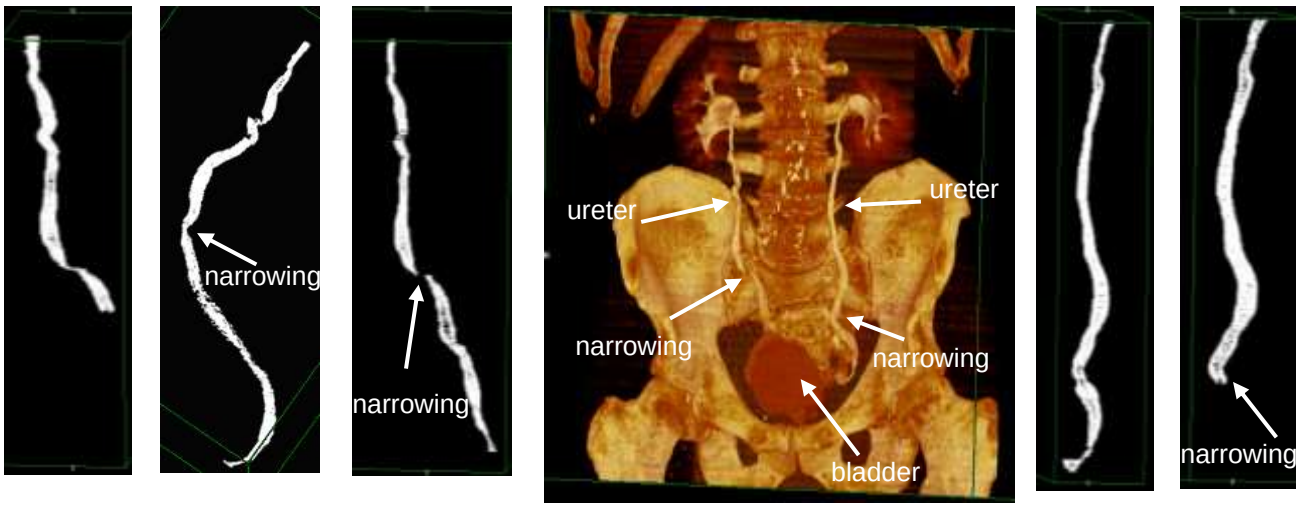

a b c d e f

Figure 9. Volume rendering of a CTU scan and the corresponding segmented left and right ureter: (a) Segmented **right** ureter of Case 2 with the **previous method** (segmented 71%, *Dist* = 1.12 mm). (b) Alternate view of the segmented **right** ureter with **COMPASS** to show the continuity at the narrowing (segmented 100%, *Dist* = 0.46 mm). (c) the segmented **right** ureter with **COMPASS** shown in the same view as in (d). (d) Volume rendering of a CTU scan (Case 2). In this case, both ureters are well opacified with IV contrast material. The ureters are less visible in the 3D volume as both ureters contained regions of narrowing. (e) Segmented **left** ureter of Case 2 with **COMPASS** (segmented 100%, *Dist* = 0.30 mm). (f) Segmented **left** ureter with the **previous method** (segmented 84%, *Dist* = 0.79 mm).

Of the 124 ureters, 120 (97%) were segmented completely (100%), 121 (98%) were segmented through at least 70% of its length, and 123 (99%) were segmented at least 50% (Fig. 10 and Table 2). With our previous method, 85 (69%) ureters were segmented completely (100%), 100 (81%) were segmented through at least 70% of its length, and 107 (86%) were segmented at least 50% (Fig. 10 and Table 2). With COMPASS, the average distance between the computer and manually tracked centerlines was 0.54 mm, and the average maximum distance was 2.02 mm for the data set of 124 ureters. Four of the 124 ureters had a distance greater than 0.75 mm and 7 had a maximum distance greater than 3.5 mm (Fig. 11 and Table 3). With the previous method, the average distance between the centerlines was 0.80 mm, and the average maximum distance was 3.38 mm. Sixty three of the

124 ureters had a distance greater than 0.75 mm and 40 had a maximum distance greater than 3.5 mm (Fig. 11 and Table 3). COMPASS improved ureter tracking length and accuracy, including regions across ureter lesions, wall thickening and narrowing of the lumen. The improvements in ureter tracking length, the distance and the maximum distance measures were all statistically significant ($p<0.0001$). The main reason for the improved COMPASS results compared to the previous method is the incorporation of the sophisticated adaptive procedure with improved decision rules and the alternative pathfinder method. Fig. 6 demonstrates the high frequency of the successful use of the adaptive procedure in the data set in order to handle the large variations in voxel gray levels and ureter diameters.

We have also performed a sensitivity analysis of the parameter settings in COMPASS (Table 4). Three key parameters: Initial Threshold, *Th,* and Th_{AC}, were varied for this analysis. Each parameter was changed ±10% and ±20% from its original value used in the baseline run (the run reported above). The results showed that the performance varied within -1.5% to 1% of the baseline values.

Table 2. Comparison of ureter tracking results using COMPASS and our previous method.

	% segmented ureters	
% ureter length successfully segmented	COMPASS	Previous method
100%	97%	69%
70% to 100%	98%	81%
50% to 100%	99%	86%

Table 3. Distance and maximum distance between the computer-tracked and manually generated ureter centerlines using COMPASS and our previous method.

	Number of ureters	
	COMPASS	Previous method
Distance > 0.75 mm	4	63
Max Distance > 3.5 mm	7	40

405

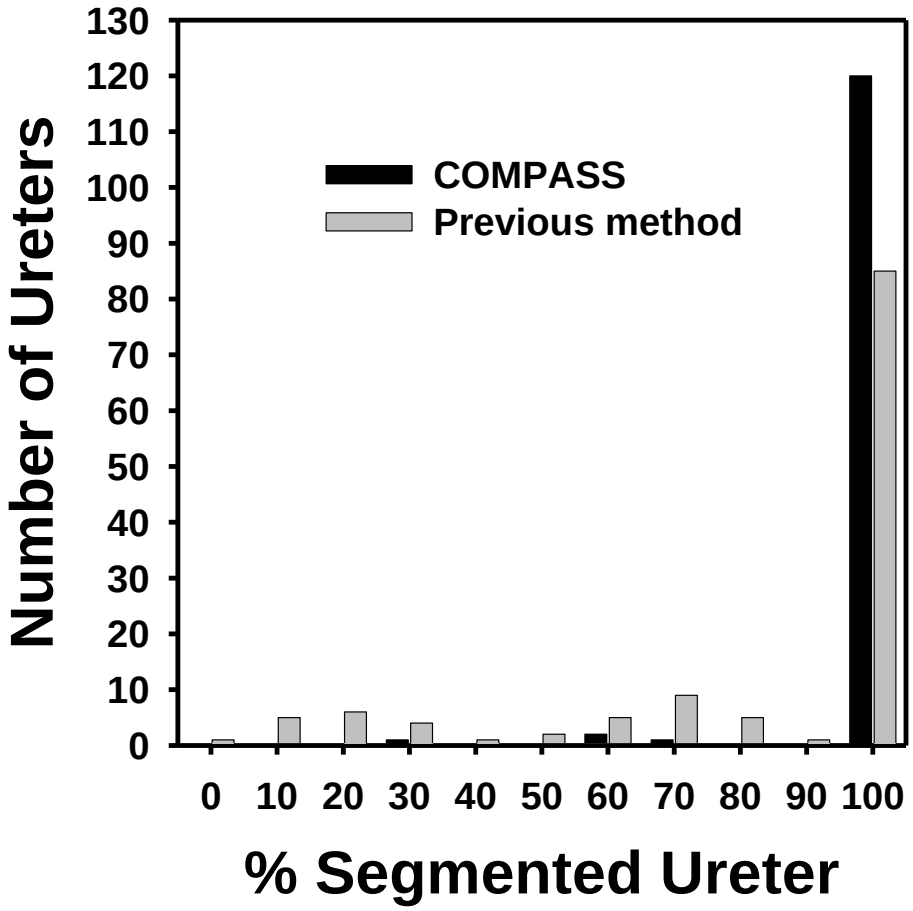

Figure 10. Comparison of the segmentation accuracy of the previous method and the current COMPASS method in terms of the percentage of the length of successfully segmented and tracked ureters.

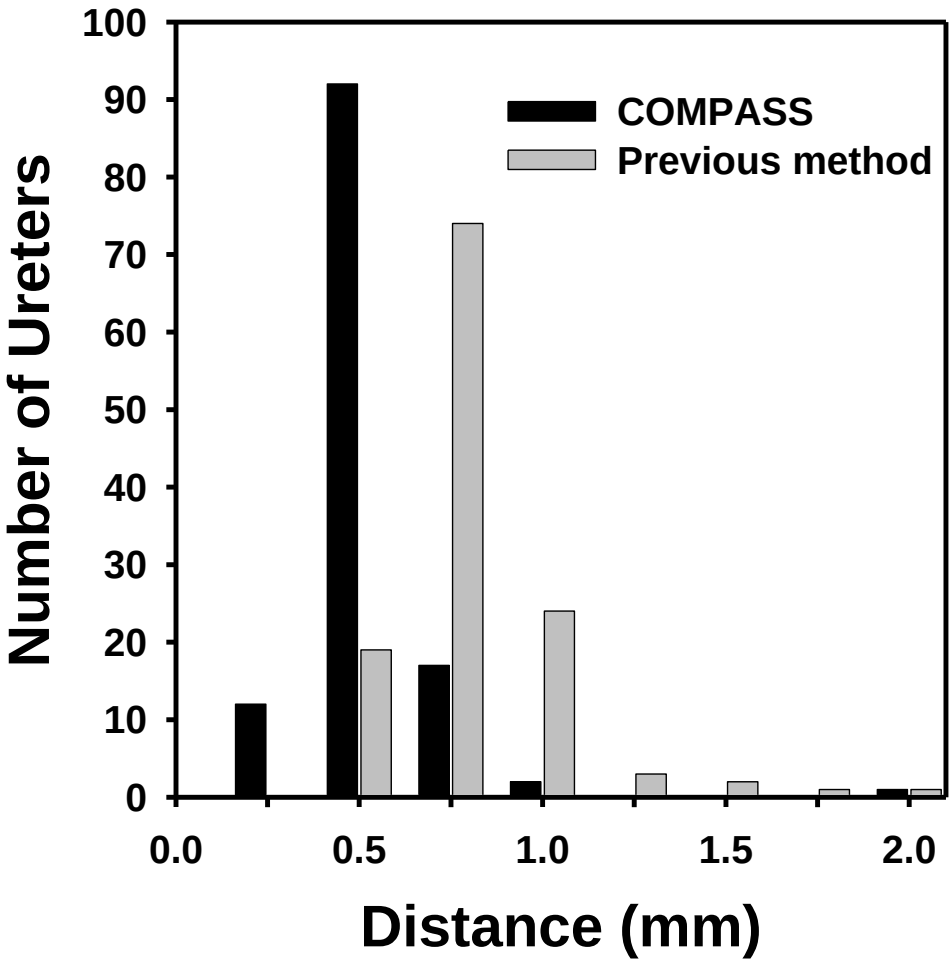

Figure 11. Comparison of the segmentation accuracy of the previous method and the current COMPASS method in terms of the distance between the computer tracked and the manually generated centerlines (*Dist*).

Table 4 Sensitivity analysis of the parameter settings in COMPASS. The three selected parameters (Initial Threshold, *Th*, and Th_{AC}) are key parameters of the system. Each parameter was changed ±10% and ±20% from its original value used in the baseline run. The reported output results were based on the 124 ureters.

	Parameters				Output		
	Initial Threshold	*Th*	Th_{AC}		Segmented ureter	Average distance	Average maximum distance
Baseline*	2000 GL (976 HU)	10.4 mm^2	0.4		98.48 %	0.54 mm	2.02 mm
Change from baseline	-20 %	0 %	0 %		0.07 %	-0.54 %	-0.52 %
	-10 %	0 %	0 %		0.03 %	-0.23 %	-1.41 %
	+10 %	0 %	0 %		0 %	-0.04 %	-0.05 %
	+20 %	0 %	0 %		0 %	-0.08 %	-0.97 %
	0 %	-20 %	0 %		0 %	-0.02 %	0 %
	0 %	-10 %	0 %		0.04 %	0.18 %	0.92 %
	0 %	+10 %	0 %		0.04 %	0.17 %	0.82 %
	0 %	+20 %	0 %		0.00 %	-0.05 %	-0.10 %
	0 %	0 %	-20 %		0.04 %	-0.05 %	0.84 %
	0 %	0 %	-10 %		0.01 %	0.24 %	0.73 %
	0 %	0 %	+10 %		0.00 %	0.19 %	-0.21 %
	0 %	0 %	+20 %		0.04 %	0.05 %	0.06 %

GL = Gray Level, HU = Hounsfield Unit, HU = GL-1024
* The baseline is the COMPASS performance with the selected parameters reported in this paper.

4. DISCUSSION

In this study, we improved our COMPASS method and evaluated its performance in a data set containing ureters in CTUs having a wide range of image quality including cases with local regions not well opacified with excreted IV contrast material. A challenge for ureter segmentation in general is the presence of regions not well opacified with excreted IV contrast material due to narrowing of the lumen caused by a ureter lesion, wall thickening or ureter muscle contraction (peristalsis). An additional challenge is the substantial variations of ureter diameter and lumen. The current

COMPASS method is shown to be more accurate and reliable for the task of ureter segmentation than the previous prototype system.

The example in Fig. 9 shows a CTU case, where both ureters have narrowing and are less visible in the rendered 3D volume (Fig. 9d). COMPASS successfully segmented both the right ureter (Fig. 9b and Fig. 9c) and the left ureter (Fig. 9e). The previous method, however, was not able to complete the segmentation for both the right (Fig. 9a) and the left (Fig. 9f) ureters. The tracking with the previous method stopped at the ureter narrowings.

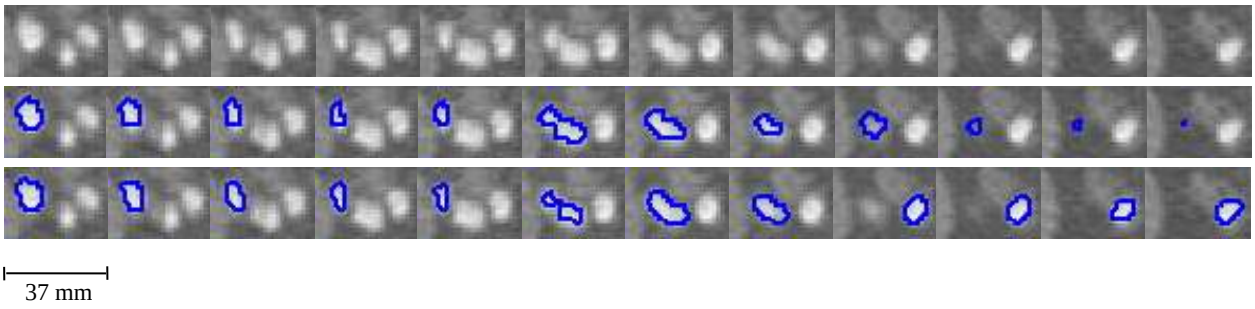

Figure 12. Comparison of segmentation and tracking of a ureter region by our previous and the current COMPASS method. (Top row): Ureter region including a kink on CTU slices. Ureter began from the slice on the left, and continued onto the slice on the right after the kink. (Middle row): The segmented edge of the corresponding ureter region by the previous method, which tracked the wrong path after the kink. (Bottom row): The segmented edge of the corresponding ureter region by the current COMPASS. The size of the ROIs is 37 mm x 24 mm.

The COMPASS segmentation of a ureter region where a kink occurred (Fig. 12) showed that COMPASS successfully performed a local search and found the correct ureter path in this more complicated situation. In contrast, the previous method was not able to track the ureter at the region with the kink and the ureter tracking terminated prematurely. A ureter region not well opacified with excreted IV contrast material due to ureter narrowing is shown in Fig. 13. This case is challenging because the ureter area is small, and the contrast difference between the ureter and the background is

very small in the narrowed region. COMPASS was able to segment the ureter region with the narrowing. The presence of ureter lesions can also create difficulty for the segmentation and tracking procedure. An example of a ureter region occluded by a malignant lesion is shown in Fig. 14. The segmentation of the ureter region by COMPASS was found to be adequate as well.

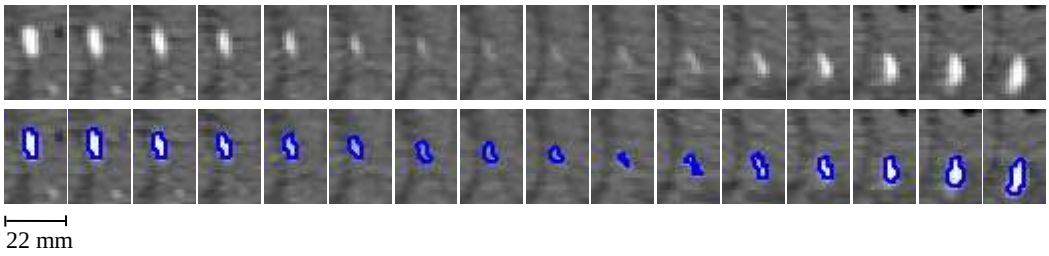

Figure 13. COMPASS segmentation and tracking of ureter region with narrowing. (Top row): Ureter region of narrowing is noted on CTU slices. (Bottom row): Segmented edge of the corresponding ureter region. The size of the ROIs is 22 mm x 33 mm.

COMPASS achieved complete segmentation in 97% of the ureters. The average distance between the COMPASS tracked and the manually generated centerlines was 0.54 mm. These results demonstrate significant improvement over the previous method and the strong promise of the improved method.

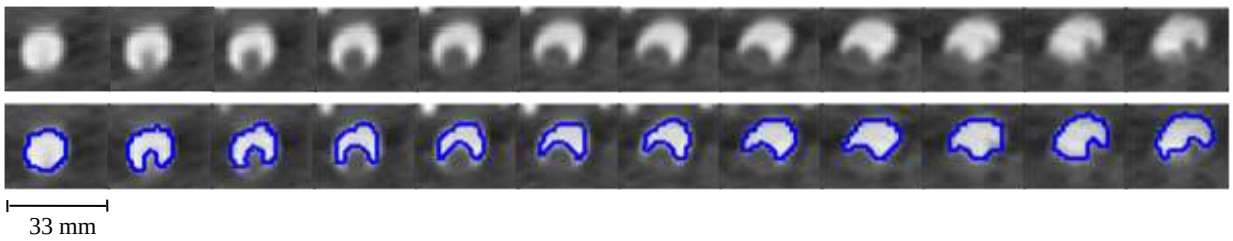

Figure 14. COMPASS segmentation and tracking of ureter region partially occluded by a malignant lesion. (Top row): Ureter region partially occluded by a malignant lesion on CTU slices. The malignant lesion blocked a large part of the ureter. (Bottom row): Segmented edge of the corresponding ureter region. The size of the ROIs is 33 mm x 26 mm.

Our sensitivity analysis demonstrated the robustness of the parameter settings of COMPASS. The adaptive procedure as designed was able to handle the relatively large variations of the contrast level and the size of the ureters. Therefore our method is likely applicable to other data sets with a wide range of contrast levels. On the other hand, the current data set did not include CTU examinations from CT scanners of different vendors or CTU imaging protocols from other institutions. The performance of the algorithms needs to be validated for these variations when such data sets are available.

There are several limitations in this study. First, the pilot data set was relatively small. We are in the process of collecting a larger database to further evaluate and improve the ureter segmentation and tracking method. Second, the starting point was manually marked so that the process was not fully automated. We will develop an automated detection method for the location where the ureter exits the kidney. Third, due to the tedious manual tracking process only one set of manually marked ureter centerlines was obtained. In the future manually marked ureter centerlines will be obtained from multiple experts in order to estimate the interobserver variability and used as reference standard for evaluation of COMPASS performance. Fourth, the ureters having regions not well opacified with contrast material could still be missed. To alleviate this problem, we are developing enhancement filters as a preprocessing step to enhance the tubular ureter structure, which is expected to improve the detectability of low contrast ureters.

5. CONCLUSION

Ureter segmentation is a crucial step in CAD systems for detection and characterization of ureter cancer and ureter wall thickening. We continue to improve COMPASS and this study demonstrated that it is a useful method for ureter segmentation in CTU scans. Our preliminary results

demonstrate the feasibility of applying COMPASS to ureter segmentation and its potential as a critical component of a CAD system for detection of ureter cancer. Study is underway to further improve the various techniques in COMPASS and evaluate the segmentation performance with a larger data set. This study is an important step towards the development of a reliable and efficient system for computer-aided detection of urinary tract cancers in CT urography.

ACKNOWLEDGMENT

This work is supported by USPHS Grant R01 CA134688.

REFERENCES

[1]"American Cancer Society, www.cancer.org 2014, "Cancer Facts & Figures 2014" " (2014).

[2]C. L. McCarthy and N. C. Cowan, "Multidetector CT urography (MD-CTU) for urothelial imaging," Radiology (P) 225, 237 (2002).

[3]M. Noroozian, R. H. Cohan, E. M. Caoili, N. C. Cowan, and J. H. Ellis, "Multislice CT urography: State of the art " British Journal of Radiology 77, S74-S86 (2004).

[4]S. A. Akbar, K. J. Mortele, K. Baeyens, M. Kekelidze, and S. G. Silverman, "Multidetector CT urography: Techniques, clinical applications, and pitfalls," Seminars in Ultrasound CT and MRI 25, 41-54 (2004).

[5]W. C. Liu, K. J. Mortele, and S. G. Silverman, "Incidental extraurinary findings at MDCT urography in patients with hematuria: Prevalence and impact on Imaging costs," American Journal of Roentgenology 185, 1051-1056 (2005).

[6]E. M. Caoili, R. H. Cohan, M. Korobkin, J. F. Platt, I. R. Francis, G. J. Faerber, J. E. Montie, and J. H. Ellis, "Urinary tract abnormalities: Initial experience with multi-detector row CT urography " Radiology 222, 353-360 (2002).

[7]E. M. Caoili, R. H. Cohan, P. Inampudi, J. H. Ellis, R. B. Shah, G. J. Faerber, and J. E. Montie, "MDCT urography of upper tract urothelial neoplasms," American Journal of Roentgenology 184, 1873-1881 (2005).

[8]L. M. Hadjiiski, B. Sahiner, E. M. Caoili, R. H. Cohan, and H.-P. Chan, "Automated detection of ureter abnormalities on multidetector row CT urography," Proc. SPIE Medical Imaging 6144, 1W1-1W7 (2006).

[9]L. M. Hadjiiski, B. Sahiner, E. M. Caoili, R. H. Cohan, C. Zhou, and H.-P. Chan, "Automated detection of ureteral wall thickening on multi-detector row CT urography," Proc. SPIE Medical Imaging 6915, 2U1-2U7 (2008).

[10]L. M. Hadjiiski, H.-P. Chan, L. Niland, R. H. Cohan, E. M. Caoili, C. Zhou, and J. Wei, "Computerized segmentation of ureters in CT urography (CTU) using COMPASS," Proc SPIE Medical Imaging 8670, 86703B: 1-7 (2013).